A Crossed Beam and *Ab Initio S*tudy of the Reaction of Atomic Boron with Ethylene

Fangtong Zhang, Xibin Gu, and Ralf I. Kaiser*

Department of Chemistry, University of Hawai'i, Honolulu, Hawaii 96822

Nadia Balucani

Dipartimento di Chimica, Università di Perugia, 06123 Perugia, Italy

Cyong H. Huang, Chih H. Kao, and Agnes H. H. Chang

Department of Chemistry, National Dong Hwa University, Hualien, 974, Taiwan

Received: November 12, 2007; In Final Form: February 9, 2008

The reaction of atomic boron, $B(^2P)$, with the simplest alkene, C_2H_4, has been investigated under single collision conditions in crossed beam experiments with mass spectrometric detection. Our experimental data clearly showed that the atomic boron versus hydrogen exchange reaction led to molecule(s) of gross formula C_2H_3B via bound intermediate(s). According to the experimentally derived fraction of the available energy released as product translational energy, we propose that an important reaction pathways is the one leading to the borirene plus atomic hydrogen and/or the one leading to ethynylborane plus atomic hydrogen. The experimental results are accompanied by electronic structure calculations of the relevant potential energy surface and RRKM estimates of the product branching ratio. According to RRKM calculations, within the limit of complete energy randomization, the three isomers borirene, $BH{=}C{=}CH_2$ and $BH_2{-}C{\equiv}CH$, are all formed, with $BH_2{-}C{\equiv}CH$ being the dominant one. The discrepancies between the trend of the product translational energy distributions and the picture emerging from RRKM estimates are a symptom that a statistical treatment is not warranted for this system.

1. Introduction

The chemical reactivity of atomic boron, $B(^2P_j)$, with inorganic and organic molecules is a fascinating subject of research that remains mostly unexplored. Apart from the fundamental interest, the elementary reactions of atomic boron are of relevance in various areas such as material sciences[1] (especially boron assisted nanotube growth[2] and the production of boron-doped diamond thin films[3,4]), high-temperature combustion,[5,6] and the synthesis of organo-boron species.[7,8] After its detection in the interstellar medium,[9] it is also conceivable that some boron chemistry can take place in those environments, provided that gas-phase reactions involving boron atoms and interstellar molecules are fast enough.

Because of its potentially high-energy release, boron has long been an interesting candidate as an energetic fuel or propellant; that has stimulated extensive research to characterize boron ignition and combustion processes. Remarkably, the lack of experimental data, particularly for high-temperature gas-phase and surface boron chemical kinetic parameters, has severely complicated the construction of realistic models for the oxidation processes.[10−12] The main problem when facing the study of elementary reactions of boron is the difficulty of preparing a significant concentration of boron atoms, because the enthalpy of sublimation is quite high (565 ± 5 kJ mol^{-1}).[13] The experimental studies on the kinetics of boron atom reactions available until 1995 have been reviewed about one decade ago.[5] An inspection of those studies shows that the reaction rate constants were known for a very limited number of reactions with oxygen-/halogen-containing molecules.[14−21]

One of the most effective ways of producing a relatively high-intensity beam of boron atoms has proved to be laser ablation.[22] This technique was applied in a series of experiments by Andrews and co-workers who investigated the reactions of boron atoms with a variety of molecules via matrix isolation techniques.[23−42] In particular, several organo-boron molecules of the generic formula BC_xH_y were identified for the first time via low-temperature infrared spectroscopy after co-deposing laser ablated boron atoms with methane,[23−25] acetylene,[26,27] ethylene,[28,29] and ethane[28,29] in an argon matrix. Those experimental studies were accompanied by *ab initio* electronic structure calculations of the relevant products and intermediates involved along the potential energy surfaces (PES)[23−30,43,44] of the reactions and showed the richness of the chemical behavior of boron atoms. However, the relatively poorly defined distribution of atomic boron velocities and electronic spin states, together with the effect of matrix trapping, made it difficult to assign the reaction mechanisms unambiguously.

An investigation at the molecular level, in a collision free environment where it is possible to observe the consequences of a single reactive event, can provide a more direct insight into the reaction mechanism.[45,46] Until very recently, the experimental investigation of boron atom reactions at the microscopic level had practically eluded the experimental techniques used in the field of reaction dynamics, which have been successfully used, instead, to investigate the reaction dynamics of most of the light second row atoms (Li, C, N, O, and F).[45,46] The only exception was the study of the reaction between the electronically excited state $B(4p,^2P)$ with molecular

10.1021/jp710810u CCC: $40.75
Published on Web 03/25/2008

hydrogen by Yang and Dagdigian.[47] Among the techniques available for the investigation of reactions under single collision conditions, the crossed molecular beam (CMB) method coupled to the mass spectrometric detection,[48] has turned out to be particularly suitable for investigating reactions giving polyatomic products that are not *a priori* predictable and/or whose spectroscopic properties are unknown.[49−57] The application of such a technique requires that it be possible to produce a beam of atomic boron of sufficient intensity to carry out product angular and velocity distribution measurements. That has been achieved in our laboratory by exploiting a pulsed beam source based on laser ablation of a boron rod. After that, a systematic investigation of $B(^2P)$ reactions with simple unsaturated hydrocarbons has been undertaken and the reaction mechanism has been elucidated for the reactions of boron with acetylene (C_2H_2),[58,59] dimethylacetylene (CH_3CCCH_3),[60] and benzene (C_6H_6).[61−64] The first report on a CMB study of an atomic boron reaction was actually on the title reaction, $B + C_2H_4$.[65] That preliminary Communication, however, only focused on the suggestion that the aromatic borirene is a primary reaction product. Because of a renewed interest on the gas-phase reactions of atomic boron, as witnessed by a recent sophisticated kinetic experiment on the title reaction,[66] as well as on B + acetylene,[67] we have reinvestigated the $B+C_2H_4$ reaction by using the same experimental technique, but with an improved crossed molecular beam apparatus. In particular, the significantly enhanced number density of the atomic boron reactant has improved the signal-to-noise ratio of the experiment and has allowed us to record the TOF spectra every 2.5° rather than every 5° as in the previous experiment. In this way, the analysis of the laboratory distribution has become more sensitive to the details of the best-fit center-of-mass functions (see below) and the related error bounds have become more stringent. Here we present a report on the new scattering data and discuss the possible atomic and molecular hydrogen loss pathways, as well as the nature of the product isomers. The experimental results are accompanied by more complete electronic structure calculations of the relevant PES and RRKM estimate of the product branching ratio.

2. Experimental and Theoretical Section

The experiment was performed by a universal molecular beam machine described in detail elsewhere.[68−70] Briefly, two well collimated supersonic beams of the reagents are crossed at 90° in a stainless-steel scattering chamber with a background pressure of about 10^{-7} Torr. A quadrupole mass filter and a Daly ion detector, preceded by a Brink-type electron impact ionizer, serve as detector of the reaction products. The detector resides in a triply differentially pumped chamber and the whole detector unit can be rotated in the collision plane around the axis passing through the collision center. In reactive scattering experiments the production of intense supersonic beams of unstable atomic or radical species is crucial. In the experiment described here a pulsed supersonic atomic boron $^{11}B(^2P)/^{10}B(^2P)$ beam was generated *in situ* via laser ablation of a solid boron rod. The boron rod is located inside the extension channel of a Proch−Trickl pulsed valve that intersects the laser beam at 90° and is attached to a motor kept in an alternating helical motion during the laser irradiation.[71] This guarantees a homogeneous consumption of the boron rod and a long-term stability and reproducibility of the source. To produce a suitable beam, the 266 nm and 30 Hz output of a Spectra Physics GCR-270-30 Nd:YAG laser was focused with 10−15 mJ per pulse on a boron rod to a spot less than 0.5 mm in diameter; the ablated boron atoms were seeded in helium and released through the Proch-Trickl pulsed valve. After the supersonic expansion, only the electronic ground state of atomic boron is populated. The helium seeded boron beam generated by high-energy laser ablation has a relatively broad velocity profile. For this reason a four-slot chopper wheel was placed between the skimmer and the interaction region.[71] The output of an infrared diode mounted at the top of the motor frame defines precisely the time zero of the experiment. When different delay times between the initial photodiode pulse and the pulsed valve are chosen, the chopper wheel operates in such a way to select distinct slices of the pulsed boron beam. In other words, the use of the chopper wheel allows selecting different beam slices characterized by a different velocity by simply delaying the opening of the pulsed valve.[71] This allows us to change the collision energy without changing the beam setup. In the case of atomic boron beams, the velocity could vary between 2030 and 2140 m s^{-1}. The experiment was performed by using a beam with a peak velocity of 2070 ± 30 m s^{-1} and speed ratio of 3.5 ± 0.2. The secondary beam of ethylene was obtained by expanding pure ethylene at room temperature and a stagnation pressure of 550 mbar in a second pulsed valve; the resulting peak velocity and speed ratio were 893 ± 15 m s^{-1} and 15.7 ± 0.2, respectively. The resulting collision energy, E_c, of the experiment was 20.1 kJ mol^{-1} calculated for the $^{11}B/C_2H_4$ system. The scattered products were recorded by the time-of-flight technique. At each angle, TOF spectra were accumulated up to 300 000 times to achieve a good signal-to-noise ratio. The recorded TOF spectra were then integrated over time and normalized to obtain a product angular distribution in the laboratory frame (LAB). Information on the chemical dynamics were gathered by fitting the TOF spectra and the LAB distributions using a forward-convolution routine.[72,73] Best fits of the TOF and laboratory angular distributions were achieved by refining the adjustable center-of-mass product angular, $T(\theta)$, and translational energy, $P(E_T)$, distributions (see below).

To compute relative energies of the $^{11}BC_2H_4$ intermediates and of the $^{11}BC_2H_3 + H$ products with respect to the separated reactants, the unrestricted B3LYP[74,75]/6-311G(d,p)[76,77] hybrid density functional theory was employed to obtain optimized geometries and harmonic frequencies; the energies are further refined with the coupled cluster[78−81] CCSD(T)/cc-pVTZ with B3LYP/6-311G(d,p) zero point energy corrections. The GAUSSIAN 98[82] and 03[83] program packages were utilized for the calculations.

3. Results and Analysis

Under our experimental conditions the reactive signal was detected at mass-to-charge ratios, m/z, of 38, 37, 36, 35, and 34 corresponding to the ions $C_2H_3{}^{11}B^+$, $C_2H_2{}^{11}B^+/C_2H_3{}^{10}B^+$, $C_2H^{11}B^+/C_2H_2{}^{10}B^+$, $C_2{}^{11}B^+/C_2H^{10}B^+$, and $C_2{}^{10}B^+$, respectively. We remind that natural boron has two isotopes of mass 11 (80%) and 10 (20%); the reported collision energy refers to the ^{11}B isotope. In the first CMB study of $B+C_2H_4$, we were not able to gain experimental evidence that the H_2 reaction channel was open. Because of the increased sensitivity of the present experimental results, special care was taken in comparing the laboratory distributions recorded for the various mass-to-charge ratios, with particular attention to the case of $m/z = 38$ and 37 distributions. The $m/z = 38$ distributions originate only from the $^{11}BC_2H_3$ product; however, the $m/z = 37$ contributions actually mirror (i) the product formed by the ^{11}B reaction through the dissociative ionization of $^{11}BC_2H_3$ to $^{11}BC_2H_2{}^+$ in the ionizer, (ii) the product of the lighter ^{10}B isotope reaction

through its parent ion $^{10}BC_2H_3^+$ and (iii) the H_2 heavy coproduct, $^{11}BC_2H_2$, if present at all. Regarding the contributions from (i) and (ii) it should be noted that, because the center of mass angles, Θ_{CM}, of the $^{11}B(^2P_j)$−ethylene and $^{10}B(^2P_j)$−ethylene systems differ by about 2.5°, the laboratory angular distributions associated with the reactions of the two isotopes are slightly displaced the one with respect to the other. As a consequence, although the TOF and laboratory angular distributions at $m/z = 38$ are fit as usual with one contribution, those at $m/z = 37$ might need two contributions, one associated to the ^{11}B reaction and one associated to the ^{10}B one. Such a procedure was indeed necessary to fit the lab data in the weakly exoergic reaction of $^{11}B(^2P_j)/^{10}B(^2P_j)$ with acetylene.[84] In the present case, however, the strongly exoergicity of the title reaction combined with the velocity and angular spreads of the boron atom beam smear out this effect. As a matter of fact, not only a single channel could fit the data obtained at $m/z = 37$, but also the LAB distributions of all the different ions formed in the ionizer were found to be superimposable (within the experimental sensitivity). This unambiguously indicates[48] that *1*) the small change in the kinematics of the $^{11}B/^{10}B$ reactions is not such to affect the shape of the LAB distributions and the best-fit functions within the sensitivity of the present experiment (to be noted that the light isotope is much less abundant than the heavy one and the dissociative ionization of $^{11}BC_2H_3$ is extensive); *2*) the only detected product in this range of masses is C_2H_3B, which partly fragments to its daughter ions in the electron impact ionizer; in particular, the H_2 loss channel does not seem to occur to a significant extent because, if the H_2 channel were open, a clear signature in the $m/z = 37$ (or smaller ion masses) distributions should be visible with respect to the $m/z = 38$ one (in this case the kinematics and exoergicity of the H-displacement and H_2 loss channels are so different that a difference would be visible either in the wings of the lab angular or in the fast rise of the TOF distributions). The signal at the m/z corresponding to the formation of the adduct, C_2H_4B, was not observed, indicating that under the single collision conditions of this experiment any possible adduct of formula C_2H_4B fragments rapidly because of its high internal energy content (the adduct $CH(BH)CH_2$ was observed in the matrix experiment[28,29,85]). Because of the better S/N, all the final measurements were carried out at $m/z = 37$. The product laboratory angular distribution together with the most probable Newton diagram showing the kinematics of the process are reported in Figure 1. The product TOF distributions are reported in Figure 2. The solid lines in Figures 1 and 2 represent the curves calculated with the best fit functions of Figure 3 (see below).

By inspecting the LAB angular distribution with the aid of the Newton diagram, we note that the products are scattered roughly in the same amount into both sides of the center-of-mass (CM) position angle, Θ_{CM}. The LAB angular distribution is relatively large (it extends for about 55°) with a broad peak. In addition, the TOF spectra display a pronounced bimodality at angles close to Θ_{CM}. These characteristics suggest that the product translational energy distribution peaks away from zero and that the fraction of available energy released in translation is significant.

The measurements are carried out in the LAB system of coordinates, but for the physical interpretation of the scattering data it is necessary to perform a coordinate transformation and move to the CM reference frame. Because of the finite resolution of experimental conditions (angular and velocity spread of the reactant beams and angular resolution of the detector), the LAB to CM transformation is not single-valued and, therefore,

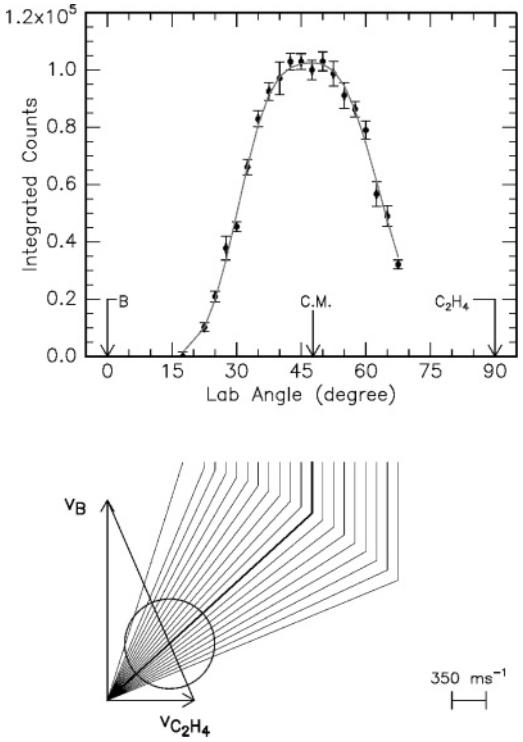

Figure 1. C_2H_3B product laboratory angular distribution (detected at $m/z = 37$) from the reaction $^{11}B(^2P) + C_2H_4(X^1A_g)$ at a relative collision energy $E_c = 20.1$ kJ mol^{-1} together with the corresponding Newton diagram. The solid line represents the angular distribution obtained from the best-fit center-of-mass functions.

analysis of the laboratory data was performed by the usual forward convoluting routine where tentative CM distributions are assumed, averaged and transformed to the LAB frame for comparison with the experimental distributions. In this iterative procedure the trial CM angular, $T(\theta)$, and translational energy, $P(E_T)$, distributions were assumed to be independent of each other. The best fit functions are shown in Figure 3. The hatched areas in Figure 3 delimit the range of CM functions that still afford an acceptable fit of the data; i.e., they represent the error bars of the present determination.

The best-fit CM angular distribution is flat (isotropic) with equal intensity in the whole angular range. However, a backward-forward symmetric angular distribution with a modest degree of polarization (the intensity ratio between $\theta = 90°$ and the two poles, $I_{90°}/I_{0°}$, should not be lower than 0.8) still afford an acceptable fit of the experimental data. Also an angular distribution with a minor peak at $\theta = 90°$ ($I_{90°}/I_{0°} \leq 1.2$) is still acceptable. In all cases, the CM angular distributions are symmetric with respect to $\theta = 90°$, thus implying that the reaction proceeds through the formation of a long-lived complex. The absence of polarization in the best-fit angular distribution is likely due to an insufficient coupling of the initial and final angular momenta. As far as the best fit $P(E_T)$ is concerned, we note that the peak position is at about 38 kJ mol^{-1}, which is quite displaced from $E_T = 0$ as it was anticipated by inspecting the characteristics of the LAB distributions. The "off-zero" peaking might indicate the presence of an exit barrier and hence tight exit transition state. The fit of both angular and TOF distributions was extremely sensitive to the rise and the peak position. However, our data were less sensitive to the tail of the $P(E_T)$, as clearly visible from the shape of the hatched area. Nevertheless, best fits could be achieved with $P(E_T)$'s extending to 150 ± 10 kJ mol^{-1}. This translates into a reaction energy of 130 ± 10 kJ mol^{-1}. This agrees well with our computed value

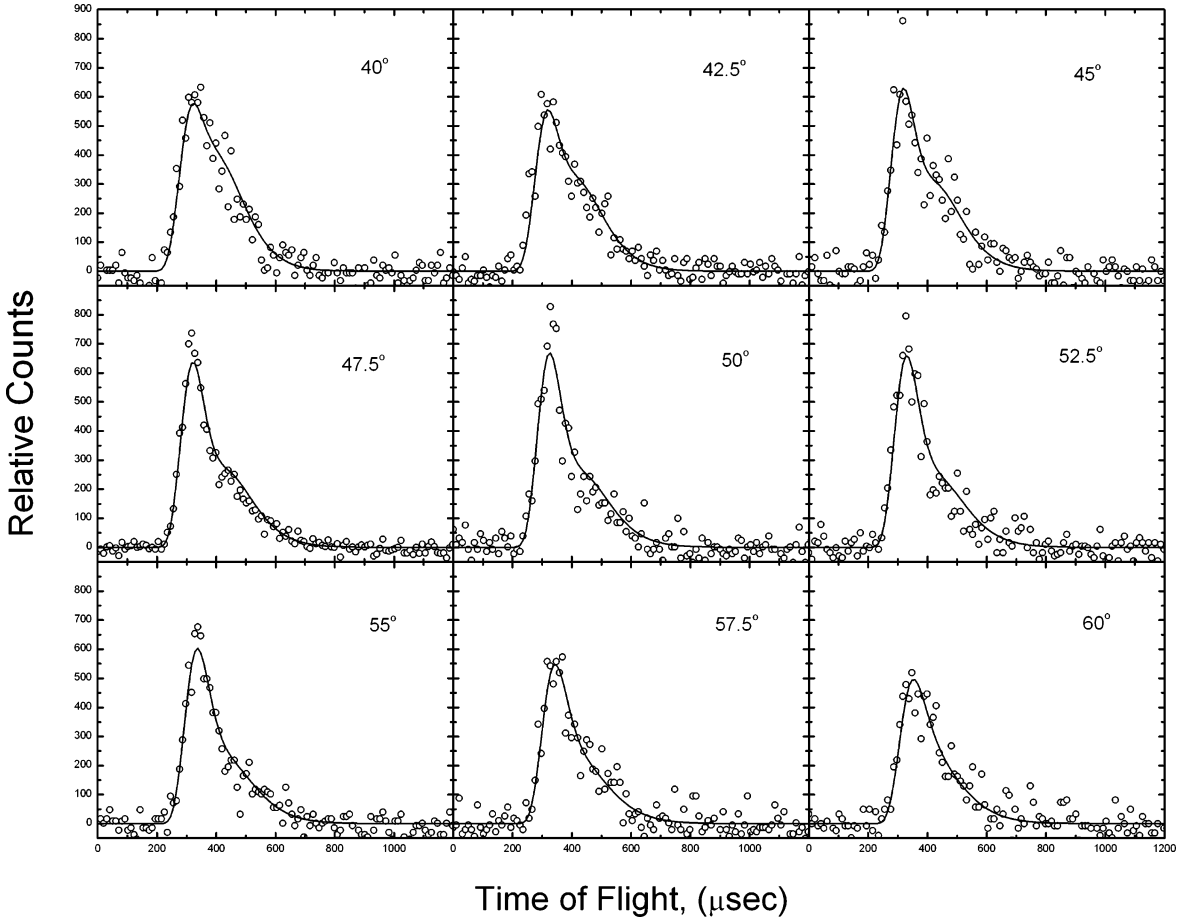

Figure 2. Time-of-flight spectra of C_2H_3B product at the indicated laboratory angles. The solid lines represent the distributions calculated from the best-fit center-of-mass functions, and the open circles represent the experimental data.

of 140 ± 10 kJ mol^{-1} (in the assumption that the molecular product is borine, see below). The average product translational energy, defined as $\langle E_T \rangle = \Sigma P(E_T)\, E_T/\Sigma P(E_T)$ is about 57 ± 4 kJ mol^{-1} corresponding to a fraction, f_T, of the total available energy ($E_{tot} = E_c - \Delta_r G°_0$) of 0.36 ± 0.03 using the theoretical value of $\Delta_r G°_0$ for the channel leading to borirene and atomic hydrogen, i.e., 140 kJ mol^{-1}.[13]

4. Discussion

Our experimental results clearly indicate that products of general formula C_2H_3B are formed through the atomic boron versus atomic hydrogen exchange channel and that the reaction pathway(s) leading to C_2H_3B products proceed(s) through the formation of a long-lived complex corresponding to a bound intermediate whose life time is longer than its rotational period. These conclusions appear to be consistent with what has been observed by Andrews et al.[28,29] and derived by Hannachi and co-workers from electronic structure *ab initio* calculations.[43] The energetics of the possible reaction channels and the relevant minima along the pathways leading to products of gross formula C_2H_3B (borirene and aliphatic isomers) and atomic hydrogen are compiled in Figures 4 −6, as derived from our new *ab initio* calculations. Note that only the formation of products **p1**−**p3** is exoergic (Figure 4); considering our collision energy of only 20 kJ mol^{-1}, the C_2H_3B isomers **p4**−**p7** are energetically not accessible under our experimental conditions. Therefore, all pathways leading to these structures have been omitted from Figure 5 for clarity.

On the basis of the potential energy surface (Figure 5), we are discussing now briefly the theoretically feasible reaction

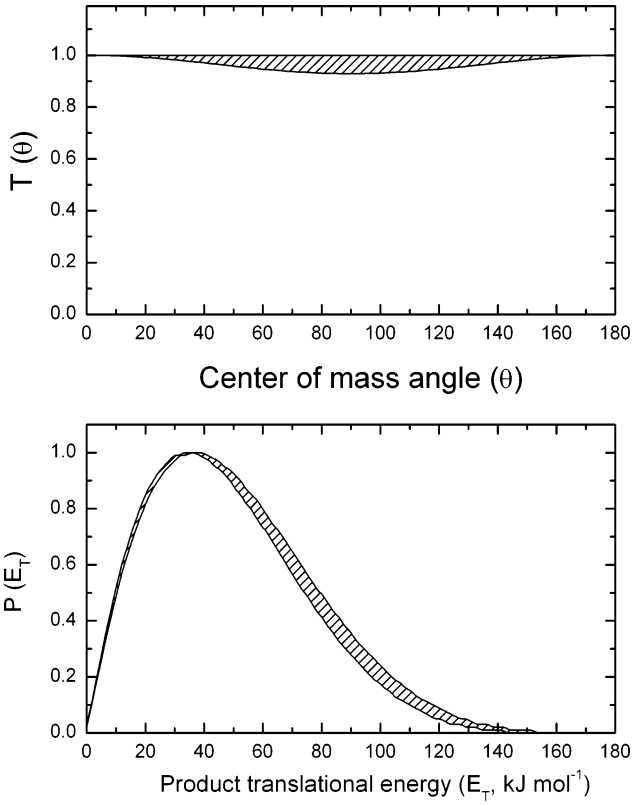

Figure 3. Best fit center-of-mass translational energy (upper) and angular distributions (lower). The hatched areas delimit the range of functions that still afford an acceptable fit of the experimental data.

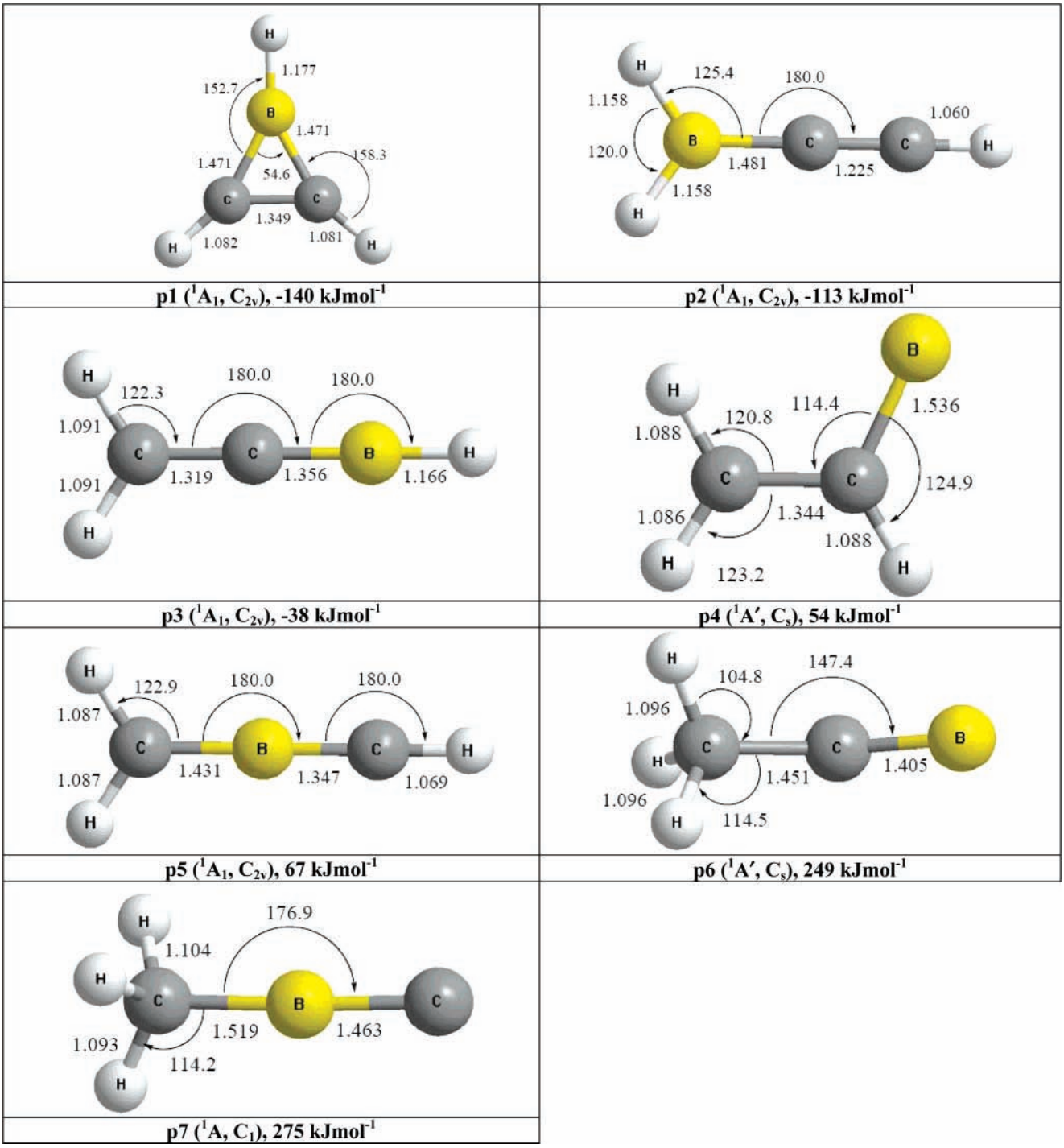

Figure 4. Structures of various $^{11}BC_2H_3$ product isomers. Bond angles and lengths are given in degrees and angstroms, respectively. Electronic states and point groups are given in parentheses. The energetics present the exoergicities of the $^{11}BC_2H_3 + H$ channel with respect to the separated atomic boron and ethylene reactants, respectively (yellow, boron; gray, hydrogen; black, carbon).

pathways and compare these data then with our experimental results. For the channel proceeding through the addition of boron atoms to the π-bond and leading to borirene also the transition states along the minimum energy path have been characterized by *ab initio* calculations. As already pointed out by previous electronic structure calculations[43,65] (B3LYP/cc-pVDZ level; zero-point energy corrected), in C_{2v} symmetry the ground state reactants correlate with a π-complex rather than directly with the borirane radical $(CH_2)_2B$ (**i1**; -194 kJ mol^{-1} with respect to the reactants in the present calculations), which actually correlates with the reactants in their electronically excited states. In C_s symmetry, there will be an avoided crossing between the two curves, so that overall the boron atom addition to form **i1** is barrier-less. Alternatively a boron atom can add to only one carbon atom of the ethylene molecule forming a weakly bound intermediate **i2** (-92 kJ mol^{-1}). On the basis of the potential energy surface and the inherent isomerization barriers, the latter prefers a ring closure to **i1** compared to an isomerization yielding **i5**. $(CH_2)_2B$ undergoes a hydrogen atom shift through a transition state located at -77 kJ mol^{-1} with respect to the reactants to form another bound intermediate, $CH(BH)CH_2$ (**i3**). Failure to observe absorption bands typical of $(CH_2)_2B$ in the matrix study[26,27] led to the conclusion that its rearrangement to $CH(BH)CH_2$ is very rapid. $CH(BH)CH_2$ (**i3**) is actually the major species observed in the matrix experiment.[26,27] Because of its high internal energy content, under the single collision condi-

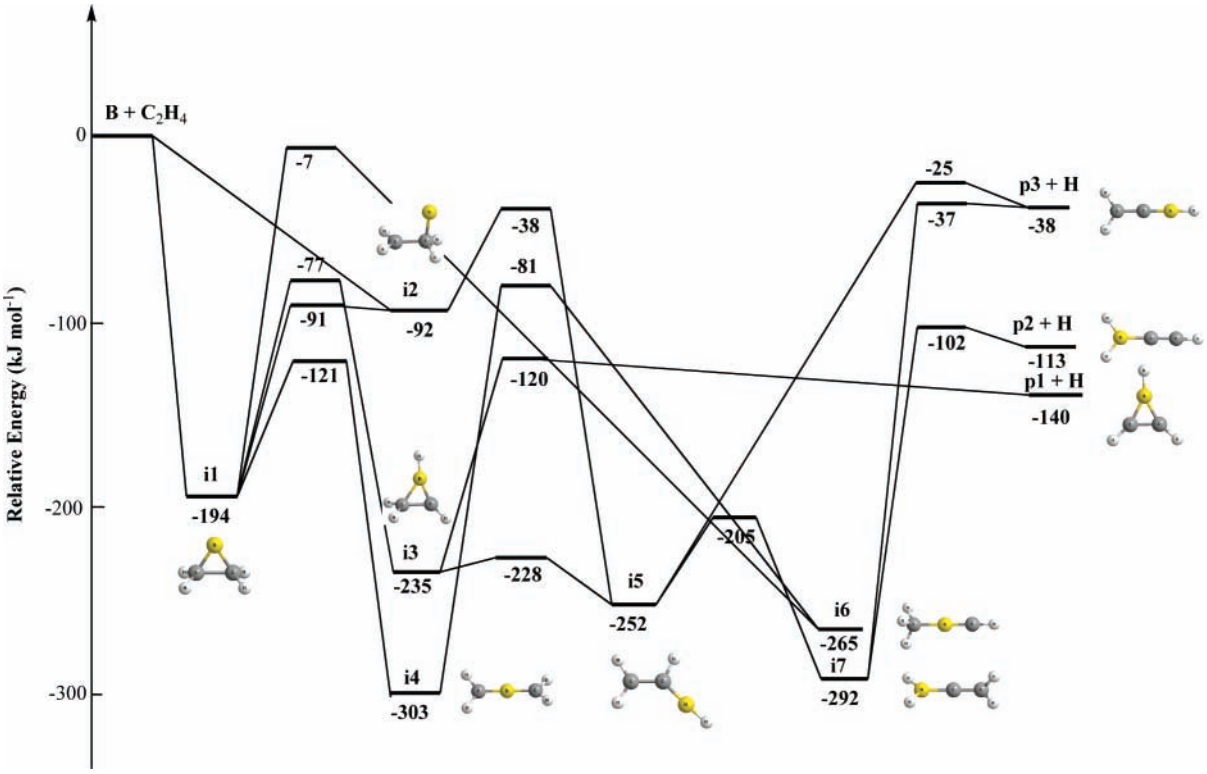

Figure 5. Schematic potential energy surface for the $B(^2P) + C_2H_4(X^1A_g)$ reaction. The intermediates, transition states, and products are characterized so that their optimized geometries and harmonic frequencies are obtained at the level of the hybrid density functional theory, the unrestricted B3LYP[74,75]/6-311G(d,p)[76,77] was employed to obtain optimized geometries, harmonic frequencies, and the energies are further refined with the coupled cluster[78−81] CCSD(T)/cc-pVTZ with B3LYP/6-311G(d,p) zero point energy corrections. The GAUSSIAN 98[82] and 03[83] program packages were utilized for the calculations.

tions of the present experiment $CH(BH)CH_2$ (**i3**) fragments to the borirene product and atomic hydrogen. According to the present *ab initio* calculations there is a small exit barrier (+20 kJ mol^{-1} with respect to products); the overall reaction to form borirene plus atomic hydrogen from the reactants is exoergic by 140 kJ mol^{-1}.

An alternative reaction pathway may proceed through the $B(^2P)$ insertion into one of the C−H bonds. A bound intermediate, the vinylborane radical, CH_2CHBH (**i5**), which lies 252 kJ mol^{-1} below reactants, was located. However, our calculations could not locate a reaction pathway of this insertion process. Failure to observe absorption bands typical of CH_2CHBH in the matrix study[26,27] led to the conclusion that it rapidly rearranges through hydrogen migration into the more stable isomer H_2BCCH_2 (**i7**). A fifth isomer with boron in central position, H_2CBCH_2 (**i4**), was calculated to be the global minimum, but its predicted absorption bands were not observed in the matrix experiment.[15] In addition, H_2CBCH_2 (**i4**) correlates only with the endoergic channel $HCBCH_2$ (**p5**) + H, which is not accessible under the present experimental conditions. The allene-like isomer H_2BCCH_2 (**i7**) can eject one hydrogen from the $-CH_2$ or $-BH_2$ group forming the singlet closed-shell molecules H_2BCCH (**p2**) and $HBCCH_2$ (**p3**), respectively. The reaction energies of these reaction channels are quite different, being −113 and −38 kJ mol^{-1}, for ethynylborane (H_2BCCH + H) (**p2**), and borallene ($HBCCH_2$ + H) (**p3**) formation, respectively. The channel leading to BH + C_2H_3 is strongly endoergic ($\Delta_r G^\circ$ = +133 kJ mol^{-1}).[13]

It should be noted that although the transition state connecting **i1** and **i4** is lower that the one leading from **i1** to **i3**, **i4** can only isomerize to **i6**. A hydrogen atom loss of the latter to form **p5** + H is energetically not accessible and hence closed. Therefore, **i6** can only react back to **i4** and hence **i1**. On the basis of the electronic structure calculations, the intermediate **i3** can, besides its hydrogen atom loss to form the borirene molecule, also isomerize very rapidly via ring opening to yield **i5**. A unimolecular decomposition of **i5** can lead to **p3** + H. But this structure can also undergo a hydrogen shift to give the second most stable intermediate **i7**. The latter can emit a hydrogen atom via a tight exit transition state forming **p2** + H and **p3** + H.

Because of the relative complexity of the system it is not trivial to determine experimentally the branching ratio among the C_2H_3B isomers formed from the $B(^2P) + C_2H_4$ reaction under our experimental conditions and hence the relative importance of **p2** and **p3** compared to the borirene molecule **p1**. The extent of the translational energy release, determined by the shape of $P(E_T)$, gives us a useful criterion through the energy conservation rule[65,67] to establish which products of general formula C_2H_3B are formed. We can determine, indeed, the value of the reaction energy, $\Delta_r G^\circ_0$, from the falloff of the $P(E_T)$ because the translational energy of the products cannot exceed the maximum total available energy $E_{max} = E_c - \Delta_r G^\circ_0$. As already noted, if we subtract E_c from the high-energy cutoff of the $P(E_T)$, the resulting reaction exoergicity is in the range of 130 ± 10 kJ mol^{-1}, a value consistent with the borirene plus atomic hydrogen formation. Because the fitting of the experimental data, however, was not very sensitive to the $P(E_T)$ falloff and the tail of the distribution could be cut by 20−30 kJ mol^{-1}, our experimental results are also compatible with the ethynylborane (**p2**) + H formation channel. The exoergicity of channel leading to borallene+H is definitively too small to account for the experimentally determined product translational energy distribution.

To address the question *which is the dominant reaction pathway?*, our experimental results were also accompanied by

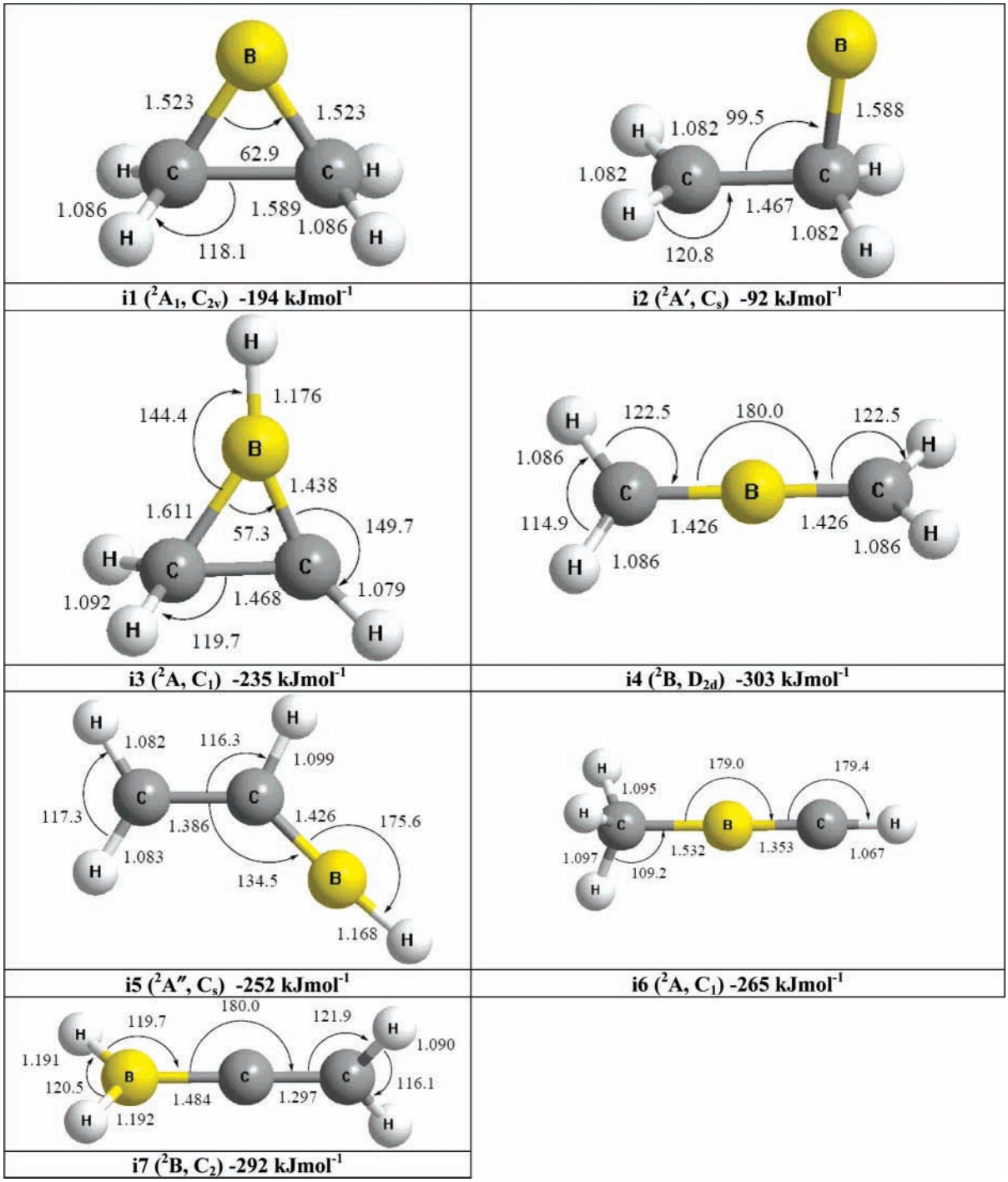

Figure 6. Structures of various $^{11}BC_2H_4$ intermediates. Bond angles and lengths are given in degrees and angstroms, respectively. Electronic ground states and point groups are given in parentheses (yellow, boron; gray, hydrogen; black, carbon).

statistical RRKM calculations including all the relevant barriers along the possible reaction pathways. The methods utilized are compiled in Reference.[85] This approach computes individual rate constants within the limit that the energy of the decomposing intermediate is completely randomized among the internal degrees of freedom. Because **i3** was identified as the central reaction intermediate, the following pathways were included in this study: **i3** → **p1** + H, **i3** ↔ **i5** ↔ **i7** → **p2** + H/**p3** + H, and **i3** ↔ **i5** → **p3** + H. This study yielded a ratio of **p1**:**p2**:**p3** of about 1.0:2.1:2.2 at our collision energy. We also conducted a computation of the energies on the CCSD(T)/cc-pVTZ level of theory with B3LYP/6-311G(d,p) zero-point energy. This results in branching ratios of **p1**:**p2**:**p3** of 1:1.8:10. Also, the loose transition state to **p3** has a significant effect on the density of states and, hence, also the rate constant of this step. Nevertheless, in both cases, product **p3** dominates. However, we should emphasize that this treatment is only valid if a complete energy randomization occurs.

The result is somewhat surprising considering that **p1** is the thermally most stable among the three and **p3** is of much higher energy. However, the relatively small yield of **p1** could be rationalized by comparing the rate constants for the critical path-splitting at **i3**, $k_{\mathbf{i3}\rightarrow\mathbf{p1}+H}$:$k_{\mathbf{i3}\rightarrow\mathbf{i5}} \sim 1{:}13$. Intermediate **i5** eventually reacts via **i7** to **p2** + **H** and **p3** + **H**. The seemingly great disadvantage of **p1** yield at first is washed away due to the fact that both **i7** and **i5** could proceed back to **i3** to a certain extent, but not enough to reverse the situation. On the other hand, the **p2**:**p3** of 1:1.25 is plainly the ratio of the rate constants $k_{\mathbf{i7}\rightarrow\mathbf{p2}+H}$:

$k_{\mathbf{i7}\rightarrow\mathbf{p3}+H}$. The magnitude of $k_{\mathbf{i7}\rightarrow\mathbf{p3}+H}$ is significantly advanced owing to a particularly loose transition state connecting **i7** and **p3** + H (19.9i cm^{-1}, 4.7 cm^{-1}, 6.5 cm^{-1}) compared to the relatively tight exit transition state involved in the formation of **p2** + H from **i7** (405.2i cm^{-1}, 44.4 cm^{-1}, 206.7 cm^{-1}) such that the density of states and hence the rate constant is elevated.

An important point has to be made here. The RRKM estimate that the **p3** + H channel is the dominant one does not reconcile well with the experimental findings, in particular with the product translational energy distribution determined in both the new and old experiments. As illustrated in section 3, the average product translational energy is 57 ± 4 kJ mol^{-1}. The maximum available energy to the product in the case of the channel **p3** + H is only 58 kJ mol^{-1}. That means that channel **p3** + H cannot be the main one, as it is unphysical that all the available energy is converted into product translation when one of the product is a polyatomic molecule. In addition, the computed loose transition state connecting **i7** to the products **p3** + H is not in line with the off-zero peaking of the product translational energy distribution, which rather indicates the presence of a tight transition state in the exit channel. Such discrepancies are certainly a symptom that a statistical treatment is not warranted for this system.

One last point needs to be commented on. According to our a*b initio* calculations, the addition pathway is barrier-less. However, the recent kinetic investigation at temperatures as low as 23 K has shown that the rate coefficient exhibits a maximum around 50 K.[65] Such an effect could be explained either by assuming that the different spin−orbit states of boron are characterized by a different reactivity or by the presence of a very small barrier (of the order of 0.2 kJ mol^{-1}) as in the case of the $B(^2P) + C_2H_2$ reaction.[66]

5. Conclusion

We have studied the reaction of atomic boron, $^{11}B(^2P)$, with the simplest alkene, C_2H_4, under single collision conditions at a collision energy of 20.1 kJ mol^{-1} in a crossed beam experiment with mass spectrometric detection. The experimental results were combined with electronic structure and statistical calculations. Our experimental data clearly showed that the atomic boron versus hydrogen exchange reaction led to molecule(s) of gross formula C_2H_3B via bound intermediate(s). We have proposed reaction pathways leading to the borirene (**p1**) plus atomic hydrogen reaction channel that has an overall reaction exoergicity of about 140 ± 10 kJ mol^{-1}. In addition, statistical calculations predict that, within the limit of a complete energy randomization, the two additional isomers, **p2** and **p3** plus atomic hydrogen can be formed. It remains to be shown in future to what extent this reaction is truly statistical.

Acknowledgment. This work was supported by the Air Force Office of Scientific Research (AFOSR; W911NF-05-1-0448). The authors would like to thank Ed Kawamura (University of Hawaii, Department of Chemistry) for his electrical work. AHHC wishes to thank the National Center for High Performance Computer in Taiwan for the support of computer resources.

References and Notes

(1) Niu, J.; Rao, B. K.; Jena, P. *J. Chem. Phys.* **1997**, *107*, 132.
(2) Hernandez, E.; Ordejon, P.; Boustani, I.; Rubio, A.; Alonso, J. A. *J. Chem. Phys.* **2000**, *113*, 3814.
(3) Xu, J.; Granger, M. C.; Chen, Q.; Strojek, J. W.; Lister, T. E.; Swain, G. M. *Anal. Chem.* **1997**, *69*, 591A.
(4) Holt, K. B.; Bard, A. J.; Show, Y.; Swain, G. M. *J. Phys. Chem. B* **2004**, *108*, 15117.
(5) Bauer, S. H. *Chem. Rev.* **1996**, *96*, 1907.
(6) Yuasa, S.; Yoshida, T.; Kawashima, M.; Isoda, H. *Combust. Flame* **1998**, *113*, 380.
(7) Ennis, L. E.; Hitchcock, A. P. *J. Chem. Phys.* **1999**, *111*, 3468.
(8) Ollivier, C.; Renaud, P. *Chem. Rev.* **2001**, *101*, 3415.
(9) Jonsson, P.; Johansson, S. G.; Fischer, C. F. *Astrophys. J.* **1994**, *429*, L45; Howk, J. C.; Sembach, K. R.; Savage, B. D. *Astrophys. J.* **2000**, *543*, 278.
(10) Brown, R. C.; Kolb, C. E.; Yetter, R. A.; Dryer, F. L.; Rabitz, H. *Combust. Flame* **1995**, *101*, 221.
(11) Zhou, W.; Yetter, R. A.; Dryer, F. L.; Rabitz, H.; Brown, R. C.; Kolb, C. E. *Combust. Flame* **1998**, *112*, 507.
(12) Zhou, W.; Yetter, R. A.; Dryer, F. L.; Rabitz, H.; Brown, R. C.; Kolb, C. E. *Combust. Flame* **1999**, *117*, 227.
(13) Linstrom, P. J.; Mallard, W. G. NIST Chemistry WebBook. In *NIST Standard Reference Database Number 69*; National Institute of Standards and Technology: Gaithersburg, MD, June 2005.
(14) Sridharan, U. C.; DiGiuseppe, T. G.; McFadden, D. L.; Davidovits, P. *J. Chem. Phys.* **1979**, *70*, 5422.
(15) DiGiuseppe, T. G.; Davidovits, P. *J. Chem. Phys.* **1981**, *74*, 3287.
(16) DeHaven, J.; O'Connor, M. T.; Davidovits, P. *J. Chem. Phys.* **1981**, *75*, 1746.
(17) DiGiuseppe, T. G.; Estes, R.; Davidovits, P. *J. Phys. Chem.* **1982**, *86*, 260.
(18) Tabacco, M. B.; Stanton, C. T.; Sardella, D. J.; Davidovits, P. *J. Chem. Phys.* **1985**, *83*, 5595.
(19) Tabacco, M. B.; Stanton, C. T.; Davidovits, P. *J. Phys. Chem.* **1986**, *90*, 2765.
(20) McKenzie, S. M.; Stanton, C. T.; Tabacco, M. B.; Sardella, D. J.; Davidovits, P. *J. Phys. Chem.* **1987**, *91*, 6563.
(21) Stanton, C. T.; McKenzie, S. M.; Sardella, D. J.; Levy, R. G.; Davidovits, P. *J. Phys. Chem.* **1988**, *92*, 4658.
(22) Jeong, G. H.; Boucher, R.; Klabunde, K. J. *J. Am. Chem. Soc.* **1990**, *112*, 3332.
(23) Hassanzadeh, P.; Andrews, L. *J. Am. Chem. Soc.* **1992**, *114*, 9239.
(24) Hassanzadeh, P.; Hannachi, Y.; Andrews, L. *J. Phys. Chem.* **1993**, *97*, 6418.
(25) Hannachi, Y.; Hassanzadeh, P.; Andrews, L. *J. Phys. Chem.* **1994**, *98*, 6950.
(26) Martin, J. M. L.; Taylor, P. R.; Hassanzadeh, P.; Andrews, L. *J. Am. Chem. Soc.* **1993**, *115*, 2510.
(27) Andrews, L.; Hassanzadeh, P.; Martin, J. M. L.; Taylor, P. R. *J. Phys. Chem.* **1993**, *97*, 5839.
(28) Lanzisera, D. V.; Hassanzadeh, P.; Hannachi, Y.; Andrews, L. *J. Am. Chem. Soc.* **1997**, *119*, 12402.
(29) Andrews, L.; Lanzisera, D. V.; Hassanzadeh, P.; Hannachi, Y. *J. Phys. Chem. A* **1998**, *102*, 3259.
(30) Galland, N.; Hannachi, Y.; Lanzisera, D. V.; Andrews, L. *Chem. Phys.* **2000**, *255*, 205.
(31) Andrews, L.; Burkholder, T. R. *J. Phys. Chem.* **1991**, *95*, 8554.
(32) Burkholder, T. R.; Andrews, L.; Bartlett, R. J. *J. Phys. Chem.* **1993**, *97*, 3500.
(33) Hassanzadeh, P.; Andrews, L. *J. Phys. Chem.* **1993**, *97*, 4910.
(34) Tague, T. J., Jr.; Andrews, L. *J. Am. Chem. Soc.* **1994**, *116*, 4970.
(35) Thompson, C. A.; Andrews, L. *J. Am. Chem. Soc.* **1995**, *117*, 10125.
(36) Lanzisera, D. V.; Andrews, L.; Taylor, P. R. *J. Phys. Chem. A* **1997**, *101*, 7134.
(37) Lanzisera, D. V.; Andrews, L. *J. Phys. Chem. A* **1997**, *101*, 824.
(38) Lanzisera, D. V.; Andrews, L. *J. Phys. Chem. A* **1997**, *101*, 1482.
(39) Lanzisera, D. V.; Andrews, L. *J. Phys. Chem. A* **2000**, *104*, 9295.
(40) Zhou, M.; Tsumori, N.; Li, Z.; Fan, K.; Andrews, L.; Xu, Q. *J. Am. Chem. Soc.* **2002**, *124*, 12936.
(41) Zhou, M.; Tsumori, N.; Xu, Q.; Kushto, G. P.; Andrews, L. *J. Am. Chem. Soc.* **2003**, *125*, 11371.
(42) Zhou, M.; Tsumori, N.; Andrews, L.; Xu, Q. *J. Phys. Chem. A* **2003**, *107*, 2458.
(43) Hannachi, Y.; Hassanzadeh, P.; Andrews, L. *Chem. Phys. Lett.* **1996**, *250*, 421.
(44) Galland, N.; Hannachi, Y.; Lanzisera, D. V.; Andrews, L. *Chem. Phys.* **1998**, *230*, 143.
(45) Casavecchia, P. *Rep. Progr. Phys.* **2000**, *63*, 355.
(46) Kaiser, R. I. *Chem. Rev.* **2002**, *102*, 1309.
(47) Dagdigian, P. J.; Yang, X. *Faraday Discuss.* **1998**, *108*, 287.
(48) Lee, Y. T. Atomic and Molecular Beam Methods. In *Atomic and Molecular Beam Methods*; Scoles, G., Ed.; Oxford University Press: New York 1987; Vol. 1, pp 553.
(49) Kaiser, R. I.; Balucani, N. *Acc. Chem. Res.* **2001**, *34*, 699.
(50) Kaiser, R. I.; Le, T. N.; Nguyen, T. L.; Mebel, A. M.; Balucani, N.; Lee, Y. T.; Stahl, F.; Schleyer, P. v. R.; Schaefer, H. F., III. *Faraday Discuss.* **2001**, *119*, 51.

(51) Balucani, N.; Stranges, D.; Casavecchia, P.; Volpi, G. G. *J. Chem. Phys.* **2004**, *120*, 9571.
(52) Balucani, N.; Alagia, M.; Cartechini, L.; Casavecchia, P.; Volpi, G. G.; Sato, K.; Takayanagi, T.; Kurosaki, Y. *J. Am. Chem. Soc.* **2000**, *122*, 4443.
(53) Garton, D. J.; Minton, T. K.; Troya, D.; Pascual, R.; Schatz, G. C. *J. Phys. Chem. A* **2003**, *107*, 4583.
(54) Willis, P. A.; Stauffer, H. U.; Hinrichs, R. Z.; Davis, H. F. *J. Phys. Chem. A* **1999**, *103*, 3706.
(55) Ran, Q.; Yang, C.-H.; Lee, Y. T.; Shen, G.; Yang, X. *J. Chem. Phys.* **2004**, *121*, 6302.
(56) Lin, J. J.; Harich, S.; Lee, Y. T.; Yang, X. *J. Chem. Phys.* **1999**, *110*, 10821.
(57) Lin, J. J.; Shu, J.; Lee, Y. T.; Yang, X. *J. Chem. Phys.* **2000**, *113*, 5287.
(58) Balucani, N.; Asvany, O.; Lee, Y. T.; Kaiser, R. I.; Galland, N.; Rayez, M. T.; Hannachi, Y. *J. Comput. Chem.* **2001**, *22*, 1359.
(59) Kaiser, R. I.; Balucani, N.; Galland, N.; Caralp, F.; Rayez, M. T.; Hannachi, Y. *Phys. Chem. Chem. Phys.* **2004**, *6*, 2205.
(60) Sillars, D.; Kaiser, R. I.; Galland, N.; Hannachi, Y. *J. Phys. Chem. A* **2003**, *107*, 5149.
(61) Kaiser, R. I.; Bettinger, H. F. *Angew. Chem., Int. Ed.* **2002**, *41*, 2350.
(62) Bennett, C. J.; Jamieson, C.; Mebel, A. M.; Kaiser, R. I. *Phys. Chem. Chem. Phys.* **2004**, *6*, 735.
(63) Bettinger, H. F. *J. Am. Chem. Soc.* **2006**, *128*, 2534.
(64) Zhang, F.; Guo, Y.; Gu, X.; Kaiser, R. I. *Chem. Phys. Lett.* **2007**, *440*, 56.
(65) Balucani, N.; Asvany, O.; Lee, Y. T.; Kaiser, R. I.; Galland, N.; Hannachi, Y. *J. Am. Chem. Soc.* **2000**, *122*, 11234.
(66) Canosa, A.; Le Picard, S. D.; Geppert, W. D. *J. Phys. Chem. A* **2004**, *108*, 6183.
(67) Geppert, W. D.; Goulay, F.; Naulin, C.; Costes, M.; Canosa, A.; Le Picard, S. D.; Rowe, B. R. *Phys. Chem. Chem. Phys.* **2004**, *6*, 566.
(68) Gu, X.; Guo, Y.; Kaiser, R. I. *Int. J. Mass Spectrom.* **2005**, *246*, 29.
(69) Gu, X. B.; Guo, Y.; Chan, H.; Kawamura, E.; Kaiser, R. I. *Rev. Sci. Instrum.* **2005**, *76*, 116103/1.
(70) Gu, X. B.; Guo, Y.; Kawamura, E.; Kaiser, R. I. *Rev. Sci. Instrum.* **2005**, *76*, 083115/1.
(71) Gu, X.; Guo, Y.; Kawamura, E.; Kaiser, R. I. *J. Vac. Sci. Technol. A* **2006**, *24*, 505. Kaiser, R. I.; Ting, J. W.; Huang, L. C. L.; Balucani, N.; Asvany, O.; Lee, Y. T.; Chan, H.; Stranges, D.; Gee, D. *Rev. Sci. Instrum.* **1999**, *70*, 4185.
(72) Vernon, M. Ph.D., University of California, Berkeley, 1981.
(73) Weiss, M. S. Ph.D., University Of California, Berkeley, 1986.
(74) Becke, A. D. *J. Chem. Phys.* **1993**, *98*, 5648.
(75) Lee, C.; Yang, W.; Parr, R. G. *Phys. Rev. B: Condens. Matter Mater. Phys.* **1988**, *37*, 785.
(76) Krishnan, R.; Binkley, J. S.; Seeger, R.; Pople, J. A. *J. Chem. Phys.* **1980**, *72*, 650.
(77) McLean, A. D.; Chandler, G. S. *J. Chem. Phys.* **1980**, *72*, 5639.
(78) Purvis, G. D., III; Bartlett, R. J. *J. Chem. Phys.* **1982**, *76*, 1910.
(79) Hampel, C.; Peterson, K. A.; Werner, H. J. *Chem. Phys. Lett.* **1992**, *192*, 332.
(80) Knowles, P. J.; Hampel, C.; Werner, H. J. *J. Chem. Phys.* **1993**, *99*, 5219.
(81) Deegan, M. J. O.; Knowles, P. J. *Chem. Phys. Lett.* **1994**, *227*, 321.
(82) Frisch, M. J.; Trucks, G. W.; Schlegel, H. B.; Scuseria, G. E.; Robb, M. A.; Cheeseman, J. R.; Zakrzewski, V. G.; Montgomery, J. A., Jr.; Stratmann, R. E.; Burant, J. C.; Dapprich, S.; Millam, J. M.; Daniels, A. D.; Kudin, K. N.; Strain, M. C. O.; Farkas; Tomasi, J.; Barone, V.; Cossi, M.; Cammi, R.; Mennucci, B.; Pomelli, C.; Adamo, C.; Clifford, S.; Ochterski, J.; Petersson, G. A.; Ayala, P. Y.; Cui, Q.; Morokuma, K.; Malick, D. K.; Rabuck, A. D.; Raghavachari, K.; Foresman, J. B.; Cioslowski, J.; Ortiz, J. V.; Baboul, A. G.; Stefanov, B. B. G.; Liu, A. L.; Piskorz, P.; Komaromi, I.; Gomperts, R.; Martin, R. L.; Fox, D. J.; Keith, T.; Al-Laham, M. A.; Peng, C. Y.; Nanayakkara, A.; Gonzalez, C.; Challacombe, M.; Gill, P. M. W. B. G.; Johnson Chen, W.; Wong, M. W.; Andres, J. L.; Head-Gordon, M.; Replogle, E. S.; Pople, J. A. *Gaussian 98*, revision A5; Gaussian, Inc.: Pittsburgh, PA, 1998.
(83) Frisch, M. J.; Trucks, G. W. Schlegel, H. B. Scuseria, G. E.; Robb, M. A.; Cheeseman, J. R.; Montgomery, J. A., Jr.; Vreven, T.; Kudin, K. N.; Burant, J. C.; Millam, J. M.; Iyengar, S. S.; Tomasi, J.; Barone, V.; Mennucci, B.; Cossi, M.; Scalmani, G.; Rega, N.; Petersson, G. A.; Nakatsuji, H.; Hada, M.; Ehara, M.; Toyota, K.; Fukuda, R.; Hasegawa, J.; Ishida, M.; Nakajima, T.; Honda, Y.; Kitao, O.; Nakai, H.; Klene, M.; Li, X.; Knox, J. E.; Hratchian, H. P.; Cross, J. B.; Bakken, V.; Adamo, C.; Jaramillo, J.; Gomperts, R.; Stratmann, R. E.; Yazyev, O.; Austin, A. J.; Cammi, R.; Pomelli, C.; Ochterski, J. W.; Ayala, P. Y.; Morokuma, K.; Voth, G. A.; Salvador, P.; Dannenberg, J. J.; Zakrzewski, V. G.; Dapprich, S.; Daniels, A. D.; Strain, M. C.; Farkas, O.; Malick, D. K.; Rabuck, A. D.; Raghavachari, K.; Foresman, J. B.; Ortiz, J. V.; Cui, Q.; Baboul, A. G.; Clifford, S.; Cioslowski, J.; Stefanov, B. B.; Liu, G.; Liashenko, A.; Piskorz, P.; Komaromi, I.; Martin, R. L.; Fox, D. J.; Keith, T.; Al-Laham, M. A.; Peng, C. Y.; Nanayakkara, A.; Challacombe, M.; Gill, P. M. W.; Johnson, B.; Chen, W.; Wong, M. W.; Gonzalez, C.; Pople, J. A. *Gaussian 03*, revision C.02; Gaussian, Inc: Wallingford, CT, 2004.
(84) Zhang, F.; Gu, X.; Kaiser, R. I.; Bettinger, H. *Chem. Phys. Lett.* **2008**, *450*, 178.
(85) Su, H.-F.; Kaiser, R. I.; Chang, A. H. H. *J. Chem. Phys.* **2005**, *122*, 074320/1.